Stable Li Metal Anode by a Hybrid Lithium Polysulfidophosphate/Polymer Crosslinking Film

*Yuming Zhao[‡], Guoxing Li[‡], Yue Gao, Daiwei Wang, Qingquan Huang, Donghai Wang**

Department of Mechanical Engineering, The Pennsylvania State University, University Park, Pennsylvania, 16802, USA.

AUTHOR INFORMATION

Corresponding Author

*Email: dwang@psu.edu (Donghai Wang)

ABSTRACT: The practical application of rechargeable lithium (Li) metal batteries has long been hindered by the unstable Li metal anode with problems like Li dendrite growth, low Coulombic efficiency (CE), and short cycle life. Here, we demonstrate a multifunctional sulfur-containing hybrid Li polysulfidophosphate and poly(2-chloroethyl acrylate) crosslinking film that can provide effective protection for Li metal anode. This film can facilitate Li metal anode generating a stable organic/inorganic hybrid solid electrolyte interphase (SEI) layer containing multiple components such as polymer-tethered organo(poly)sulfide, inorganic Li polysulfidophosphate, Li sulfides, and Li salts. Thanks to this hybrid robust SEI layer, dendrite-free Li deposition and stable cycling of Li metal anode can be achieved (e.g. CE >98.7% over 950 cycles). We demonstrated this Li protection technique enables both the protected Li metal anode and Li-metal-free anode cycling with significantly improved CEs and stability in full cells using $LiFePO_4$ (~2.4 mAh/cm^2) cathode.

TOC GRAPHICS

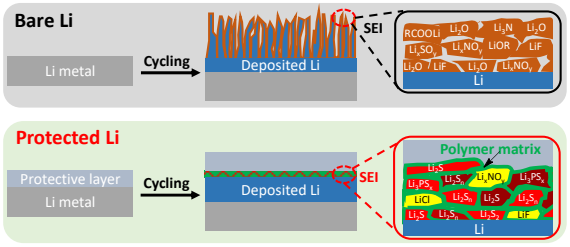

Lithium (Li) metal with high theoretical specific capacity (3860 mAh g^{-1}) and the lowest electrochemical potential (-3.04 V vs standard hydrogen electrode), has been considered as an ideal anode material for the next generation high energy density storage systems.[1, 2] However, the practical deployment of Li metal anode has long been hindered by its high reactivity to liquid electrolyte, accompanied by problems like Li dendrite growth, low Coulombic efficiency (CE) and short cycle life.[3, 4] Usually, a solid electrolyte interphase (SEI) is formed on the surface of Li metal anode, serving as a protective layer to prevent its further reaction with liquid electrolyte and its consumption.[5] Typically, this SEI layer is poorly formed and incapable of withstanding the enormous volume fluctuations of Li metal during Li plating/stripping cycling, leading to generation of cracks in the SEI layer and the formation of mossy, needlelike dendritic Li. Besides, the repeated breakdown and formation of SEI layer gives rise to problems like accelerated depletion of electrolyte, dramatically increased internal resistance, low CE and short cycle life.[6, 7] To solve these problems, it is necessary to explore and discover an appropriate approach to regulate or stabilize the SEI layer for Li metal anode. So far, two strategies using functional electrolyte additives[8-10] or fabricating mechanically robust protective layer (or artificial SEI)[11-13] have been widely adopted to regulate the SEI layer for Li metal anode and to suppress the Li dendrite growth. However, the electrolyte-derived SEI layer is still very fragile and prone to breakage, especially at high current density and areal capacity or during long-term cycling.[14-16] The mechanically robust layers can provide flexibility to accommodate the volume fluctuations during Li plating/stripping, however, they are unable to completely prevent the penetration by Li dendrite and reaction of liquid electrolyte with Li metal, resulting in continuous consumption and fast depletion of the liquid electrolyte.[11, 17-20]

Recently, reactive polymeric composite layers have been reported to be an effective approach to improve the SEI layer and enable stable cycling of Li metal anode, benefited from the synergetic construction of robust SEI layer from both functional groups in the polymer and liquid electrolyte.[21-27] The formation of SEI layer using the reactive polymer typically involves two steps. First, the polymer layer, attached to the Li surface, occupies the surface active sites by chemically reacting with Li. Second, the attached polymer then electrochemically decomposes at the interface, accompanied by the liquid electrolyte decomposition, to form the reinforced SEI layer on Li metal. For example, we reported use of a cyclic ether based reactive polymer to provide effective protection for Li metal anode and enable an excellent cycling performance of Li metal batteries.[21] Thereafter, our group further developed use of a sulfur-rich polymer as electrolyte additive to regulate the SEI layer for Li metal anode, such that a hybrid SEI containing mainly organo(poly)sulfide and inorganic sulfides (e.g. Li_2S/Li_2S_2) can be generated on the surface of Li metal anode.[22, 28] Particularly, the organo(poly)sulfide components can increase the flexibility of the SEI layer, which is helpful to withstand the enormous volume fluctuations during Li plating/stripping cycling. Meanwhile, the inorganic sulfides can contribute to reinforce the SEI layer so as to enable a dendrite free Li deposition. However, in this system, the insolubility of the sulfur-rich polymer makes it difficult to disperse uniformly in the liquid electrolyte and easy to precipitate during storage. In addition, the generated organo(poly)sulfide possess a low Li ion conductivity, which is unfavorable for Li ion transport through the interface.

To address the challenges in using the sulfur-rich polymer to manipulate the SEI for Li metal, here we propose an in-situ chemically cross-linked, multifunctional sulfur containing polymer (MSCP) as a protective layer, utilizing both advantages of the functional polymeric groups and the inorganic sulfur-containing groups, to improve the SEI layer for Li metal anode. The MSCP

polymer film is designed and fabricated on the surface of Li metal anode, as shown in **Figure 1A**. Two key features in the MSCP polymer are the incorporation of lithium polysulfidophosphate (Li_3PS_x denoted as LiPSP) components in inorganic sulfur containing group and in-situ crosslinking of the LiPSP and polymer into a protective film with a benefit potentially for large scale fabrication. Due to the presence of LiPSP components, the Li_3PS_x is generated along with polymeric components and inorganic Li sulfides in the organic/inorganic hybrid SEI layer, and the presence of Li_3PS_x is beneficial for Li-ion transport in the SEI layer due to its higher Li-ion conductivities than Li sulfides.[29, 30] The coexistence of multiple components in the hybrid SEI generated from the MSCP, including polymer-tethered organo(poly)sulfide, inorganic Li_3PS_x and lithium sulfides, and Li salts, renders the dense SEI layer durable to withstand the volume fluctuations of Li metal during cycling and inhibit the growth of Li dendrite (**Figure 1B**). In addition, the mechanically robust MSCP film, due to its crosslink feature, also contributes to its long-term cycling stability. The electrochemical evaluation demonstrates that dendrite-free Li deposition and excellent cycling performance of Li metal anode can be achieved with average CE above 98.7% over 950 cycles at a current density of 1 mA cm^{-2} and areal capacity of 1 mAh cm^{-2}, and with average CE above 98.2% over 130 cycles even at a higher current density of 4 mA cm^{-2} and areal capacity of 4 mAh cm^{-2}. The full cell using $LiFePO_4$ (LFP, ~2.4 mAh/cm^2) as cathode and the protected Li metal as anode also exhibits a superior capacity retention (>89% after 500 cycles) with high average CE of 99.9%.

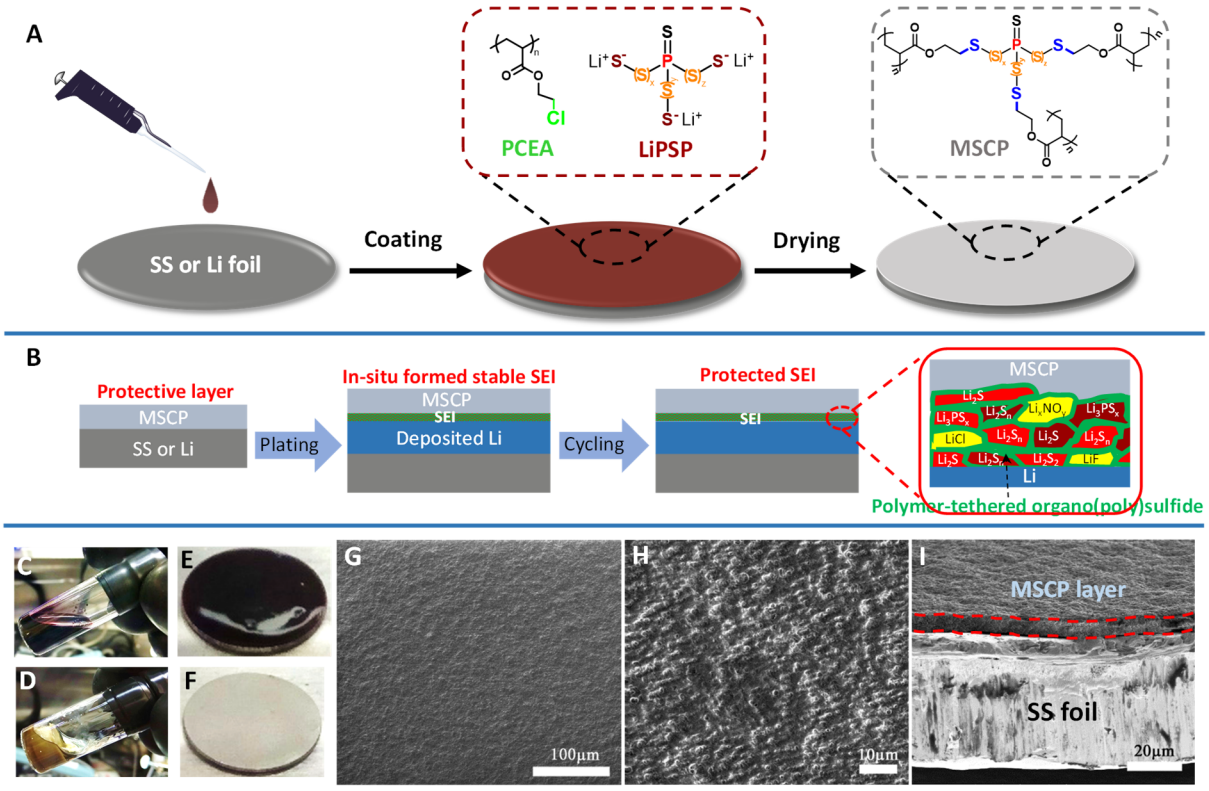

Figure 1. (A) Schematic illustration of fabricating MSCP protective layer on stainless steel (SS) or Li foil. (B) Schematic illustration of Li plating/stripping behavior and the in-situ formed organic/inorganic hybrid SEI layer by using MSCP protective layer. Optical images of (C) the as-mixed LiPSP and PCEA solution and (D) after staying for 10 h at room temperature. Optical images of (E) the as-mixed LiPSP and PCEA solution dropped on SS foil and (F) after drying under vacuum at room temperature. (G and H) Top view and (I) side-view SEM images of the as-prepared MSCP film on SS foil.

The MSCP protective layer was prepared using an in-situ crosslinking reaction between LiPSP and a chlorine rich polymer poly(2-chloroethyl acrylate) (PCEA), as shown in **Figure 1A**. LiPSP was prepared by a reaction of elemental sulfur (S_8) with lithium thiophosphate (Li_3PS_4) in a stoichiometric ratio in 1-methyl-2-pyrrolidinone (NMP) solvent.[30] PCEA was prepared by a free

radical polymerization of monomer 2-chloroethyl acrylate in NMP solvent with azobisisobutyronitrile (AIBN) as an initiator and its chemical structure was characterized by proton nuclear magnetic resonance spectroscopy (^{1}H-NMR) (**Figure S1**). As shown in **Figure 1C** and **D**, the as-mixed solution of LiPSP and PCEA is dark red and turns into pale yellow gel after staying at room temperature for 10 h, indicating a crosslinking reaction between LiPSP and PCEA. To fabricate a MSCP protective layer, 50 μL of LiPSP and PCEA mixed solution was dropped onto a stainless steel (SS) foil to form a liquid dark red film, followed by drying under vacuum immediately for 24 h. After drying, the dark red liquid film (**Figure 1E)** turns into a uniform off-white solid MSCP film (**Figure 1F**). The thickness optimization of MSCP protective layer was achieved by controlling the amount of polymer solution followed by electrochemical tests of half-cells, as shown in **Figure S2**. The optimized MSCP film appears to have a uniform coating layer with a thickness of around 6.0 μm from scanning electron microscopy (SEM) investigation (**Figure 1G-I**). The crosslinking between LiPSP and PCEA was further verified by X-ray photoelectron spectroscopy (XPS) characterization showing the formation of LiCl salt and the C-S bond, as shown and discussed in **Figure S3**. The hybrid MSCP film exhibits a high elastic modulus of 1.585 ± 0.223 GPa and hardness of 0.06 ± 0.011 GPa evaluated by the nanoindentation technique (**Figure S4**), which can facilitate accommodating the volume change of Li metal anode and mechanically strengthen as-generated hybrid SEI layer for effective Li protection during cycling.

The Li deposition on SS foil with and without an MSCP protection film was conducted using a two-electrode configuration cell with Li metal as a counter electrode. The morphologies of the deposited Li were characterized by SEM. As shown in **Figure 2A-C**, Li deposition on bare SS foil shows an accumulated Li dendrite morphology with a coarse and fluffy cross section. This is

because the electrolyte-induced SEI layer is too fragile to withstand the huge volume fluctuations during Li plating/stripping cycling, leading to the SEI breakage and the growth of Li dendrite.[31] For Li deposition on the MSCP film protected SS foil, the MSCP layer on the top surface keeps intact and uniform after cycling (**Figure 2D** and **E**). Also, a sandwich cross-section structure can be observed that consists of a top layer of the MSCP film, a middle layer of the deposited dense Li, and a bottom layer of the SS foil (**Figure 2F**). After stripping, the protective layer on SS foil remains intact, as shown in **Figure S5**. Moreover, even after 100 cycles, the deposited Li is still covered by the protective layer showing a sandwich cross-section structure (**Figure S6**). The results demonstrate that the MSCP protective layer can provide an effective protection for Li metal anode and enable a dendrite-free Li plating/stripping after a long-term cycling.

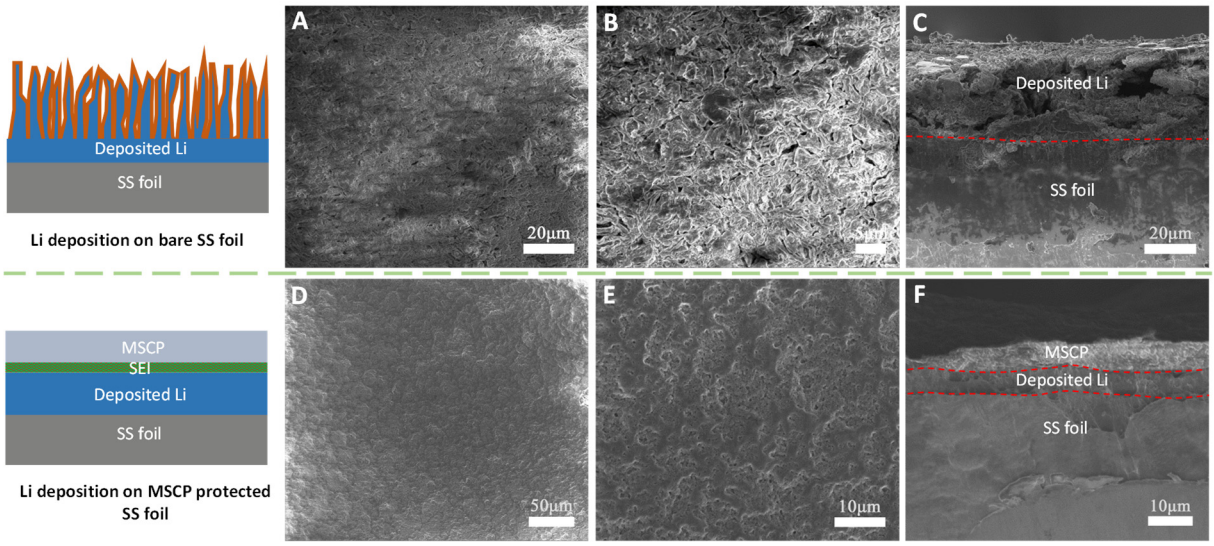

Figure 2. (A and B) Top-view and (C) side-view SEM images of deposited Li on bare SS foil after 10 cycles. (D and E) Top-view (F) side-view SEM images of deposited Li on MSCP protected SS foil after 10 cycles. The cells were cycled at 2 mA cm^{-2} and 2mAh cm^{-2}.

In order to better understand the protection of the MSCP film for Li metal anode, chemical components of the SEI layer (MSCP-SEI) using MSCP protection film has been investigated by the XPS characterization and compared with control SEI in cells using bare SS foil. As shown in **Figure 3**, the chemical components of MSCP-SEI and control SEI layers are analyzed through the deconvoluted S 2p, P 2p, Cl 2p, Li 1s, C 1s, F 1s and N 1s XPS spectra. In MSCP-SEI, peaks at 160.5 and 161.3 eV in S 2p spectra (**Figure 3A**) can be ascribed to the inorganic sulfide components Li_2S, Li_2S_2 and Li_3PS_x.[22, 32] The existence of Li_3PS_x components can be confirmed from the P 2p spectra (**Figure 3B**).[32] The peak at 163.3 eV in S 2p spectra corresponding to S-S and C-S bonds can be ascribed to the inorganic polysulfides (Li_2S_n, $n\geq3$) and the polymer-tethered organo(poly)sulfide (the structure can be found in **Figure S7**).[22, 33, 34] The existence of polymer-tethered organo(poly)sulfide can also be verified from the C-S bond in C 1s spectra (**Figure S8A**).[35] In addition, inorganic salts such as LiCl, LiF and Li_xNO_y can be observed from Cl 2p (**Figure 3C**), F 1s (**Figure S8 B**) and N 1s (**Figure S8 C**) spectra, respectively.[31, 36, 37] The existence of multiple Li salts and Li sulfides can be also confirmed from the Li 1s spectra (**Figure 3D**).[36, 38, 39] In contrast, control SEI mainly contains inorganic salts such as Li_xSO_y, ROLi, RCOOLi, Li_2O, Li_xNO_y, and LiF (**Figure 3E-H** and **Figure S8 D-F**), as observed in typical electrolyte-derived SEI layers.[31, 37, 38] We further compared the contents of elemental composition between MSCP-SEI and control SEI, as shown in **Figure 3I**. The MSCP-SEI shows a higher content of C (36.82%), S (10.16%), P (3.48%) and Cl (1.19%), but a lower content of O (28.24%), Li (16.52%), N (1.51%) and F (2.08%), compared with that of control SEI (C 11.63%, S 3.16%, P 0%, Cl 0%, O 42.14%, Li 35.44%, N 11.63% and F 5.83%). The higher content of C in MSCP-SEI implies polymer dominant SEI rather than inorganic-dominant SEI, which is attributed to a significant participation of MSCP into the SEI formation. The contribution of

MSCP to MSCP-SEI also manifest at a higher content of sulfur species in MSCP-SEI due to chemical/electrochemical decomposition of the sulfur species from MSCP at the interfaces. The higher content of P species in MSCP-SEI particularly indicates the presence of Li_3PS_x species in the SEI. On the other side, the lower content of N and F in MSCP-SEI indicates an alleviated decomposition of LiTFSI and $LiNO_3$ salts by using MSCP, as LiTFSI is the only source of F and both LiTFSI and $LiNO_3$ are the only source of N in the electrolyte. Furthermore, the lower content of Li and O in MSCP-SEI indicates a reduced consumption of the Li salt as well as electrolyte by using MSCP.[40] Collectively, the results indicate that an organic/inorganic hybrid SEI layer, containing polymer-tethered organo(poly)sulfide, inorganic Li_3PS_x and Li sulfides, and Li salts, can be in-situ generated by the MSCP protective layer. The soft polymer-tethered organo(poly)sulfide are more favorable to improve the flexibility of SEI layer[22, 28], while the multicomponent inorganic Li compounds can serve to reinforce the SEI layer.[31, 37] Particularly, the existence of Li_3PS_x components may contribute to an SEI layer with improved Li-ion conducitivity.[29, 30] All of these advantages of MSCP-SEI may make the MSCP an effective protective layer for Li metal anode.

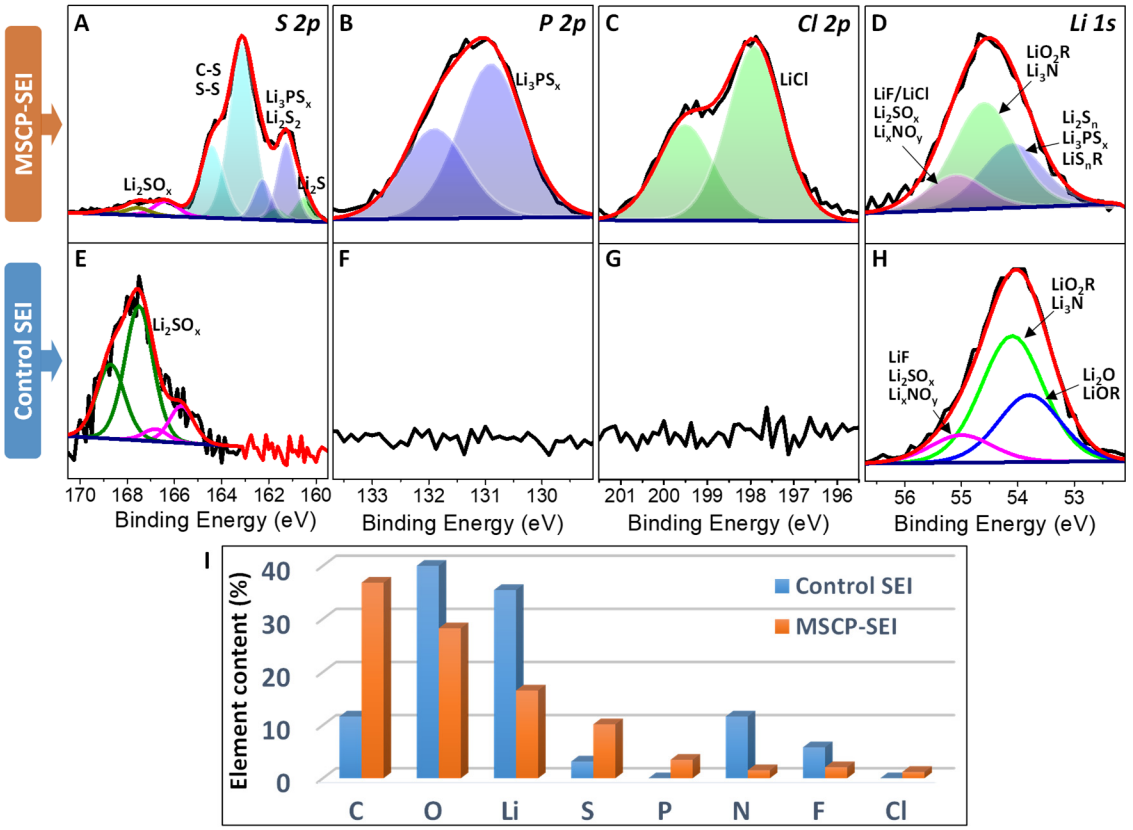

Figure 3. S 2p, P 2p, Cl 2p and Li 1s XPS spectra of (A-D) MSCP-SEI and (E-H) control SEI. (I) Elemental composition comparison of control SEI and MSCP-SEI calculated based on the XPS spectra.

Next, we evaluate the electrochemical cycling performance of Li deposition using the MSCP protection layer to illustrate its advantages. In our experiment, Li metal was electrodeposited on SS foil with and without an MSCP protection film in a two-electrode cell using Li metal as a counter electrode at different deposition conditions. As shown in **Figure 4**, compared with the fast drop of CEs using bare SS foil, cells using MSCP protected SS foil can maintain high CEs for a prolonged cycle life. Specifically, an average CE of 98.7% for over 950 cycles at 1 mA cm^{-2} and 1 mAh cm^{-2} (**Figure 4A**), and an average CE of 98.5% for over 460 cycles at 2 mA cm^{-2}

and 2 mAh cm^{-2} (**Figure 4B**) can be achieved for cell using the MSCP protected SS foil. Even at higher capacities of 3 mAh cm^{-2} and 4 mAh cm^{-2}, very stable cycling can also be achieved (**Figure 4C** and **D)**, respectively. In contrast, no stable cycling can be achieved for cells using bare SS foil at higher capacity and current density (**Figure 4D** and **S9 B-D**). In addition, a comparison of voltage profile and electrochemical impedance spectra (EIS) between cells with bare SS foil and MSCP protected SS foil can further demonstrate a stable and low-impedance MSCP-SEI layer, as shown in **Figure S10** and **S11**.

We also found the hybrid, crosslinking feature of the MSCP layer combining the polymeric and the inorganic components plays an important role in achieving the stable SEI and superior electrochemical performance. The cycling performances are compared between cells with an MSCP protected SS foil and with either a polymer PCEA or an inorganic LiPSP protected SS foil. As shown in **Figure S12A**, the cell with a PCEA protected SS foil shows a fast drop of CE after around 120 cycles. This is probably because its linear chemical structure and the dissolution/swelling properties in the electrolyte prevent it from forming a stable SEI and suppressing Li dendrite growth. In parallel, the cell with LiPSP protected SS foil shows a stable cycling over ~230 cycles, which is much better than the cell with a bare SS foil, though still worse than the cell with an MSCP protected SS foil. The improved cycling stability with LiPSP protected SS foil can be ascribed to the SEI enhancement by lithium polysulfide for Li metal anode.[22, 31, 37] However, when the cells are cycled at 4 mA cm^{-2} and 4 mAh cm^{-2}, poor CEs were achieved for cells with a LiPSP protected SS foil (**Figure S12B**), which is in sharp contrast with the highly stable cycling of cell with a MSCP protected SS foil (**Figure S9D**). The superior cycling stability of cell with MSCP protected SS foil can be ascribed to its in-situ formed very stable and robust SEI layer, and its alleviated decomposition of electrolyte. Furthermore, since

the SEI layer is in-situ generated and stays covered by the unreacted part of MSCP protective layer, we believe that this protected SEI layer will also contribute to the stable cycling of Li metal anode. The significantly improved cycling performance of cells with a MSCP protective layer at different cycling conditions (**Figure 4** and **S9**) were also summarized in **Table S1** in Supporting Information and compared with other state-of-art Li metal anode protection techniques. Our strategy utilizing the MSCP as a protective layer for Li metal anode shows superior performance among strategies using Li_2S_n or sulfur-rich polymer as additives.

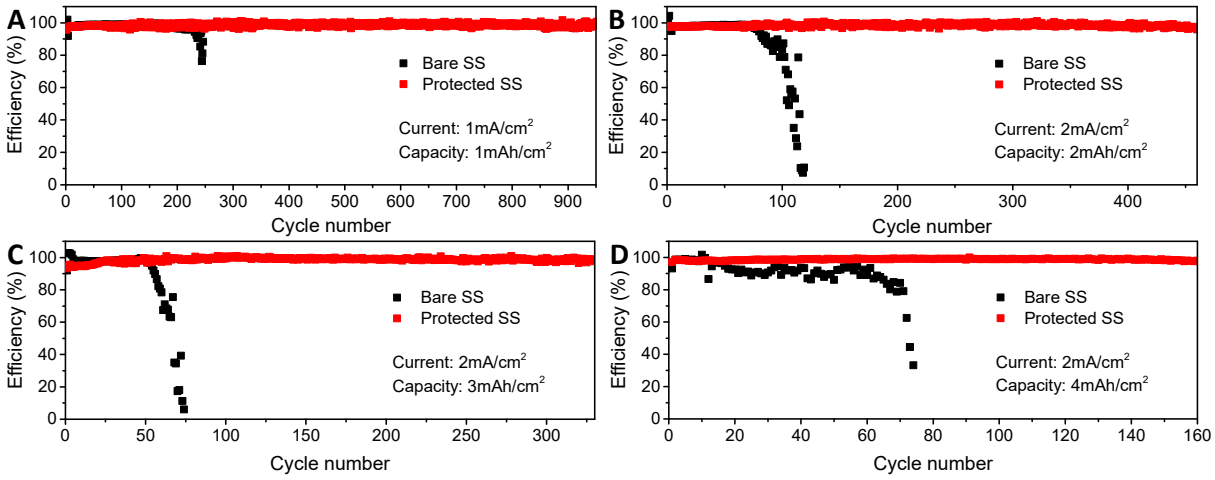

Figure 4. CEs of cells using bare (black) and MSCP protected (red) SS foil versus cycle number at (A) 1 mA cm^{-2} and 1 mAh cm^{-2}, (B) 2 mA cm^{-2} and 2 mAh cm^{-2}, (C) 2 mA cm^{-2} and 3 mAh cm^{-2}, and (D) 2 mA cm^{-2} and 4 mAh cm^{-2}.

The excellent performance of MSCP for Li metal deposition was also demonstrated by the direct coating on Li metal surface and testing in a Li||Li symmetric cell configuration. **Figure 5A** shows voltage profiles as a function of time of two Li||Li symmetric cells using bare or MSCP protected Li metal foils. The cell using bare Li metal foils shows a very high voltage

overpotential (> 230 mV) during cycling and becomes short-circuited after about 80 h as indicated by the exacerbated voltage fluctuation. In contrast, the cell using MSCP protected Li metal foils shows lower voltage overpotential (< 120 mV) and stable cycling for more than 800 h without an obvious voltage fluctuation. Finally, the MSCP protection for Li metal anode was further evaluated in full cells using LFP (~2.4 mAh/cm^2) cathode and the MSCP protected Li metal anode. As shown in **Figure 5B**, the LFP cell with bare Li metal anode shows very fast capacity fading, less than 80% capacity retention after only 100 cycles, and a gradually increased voltage polarization (**Figure S13A**). This can be ascribed to increased impedance caused by the unstable and accumulated SEI between Li metal anode and the liquid electrolyte. In contrast, the cell with MSCP protected Li metal anode shows significantly increased cycling performance with a capacity retention of ~89.4% even after 500 cycles and an improved average CE of ~99.9%. Meanwhile, it shows a very stable charge-discharge voltage profile with very limited increase of voltage polarization (**Figure S13B**) owing to the stable MSCP-SEI in the protected Li anode. Furthermore, we found that an anode-free cell using MSCP protected SS foil as anode and LFP as cathode shows remarkably improved cycling stability than that in a bare SS foil anode-free cell. The cell with bare SS foil shows a very fast capacity drop (less than 60% capacity retention within 15 cycles and almost zero after 100 cycles) and significantly decreased CE (98.18% at the first cycle to 93.89% after 120 cycles) (**Figure 5C**). Contrastingly, the cell with MSCP protected SS foil shows more stable cycling with 62.9% capacity retention after 60 cycles and high CE of 99.27% even after 120 cycles (**Figure 5C**). From the corresponding charge-discharge profile of two cells (**Figure S14**), remarkable voltage polarization was observed for the anode-free cell with bare SS foil in contrast to the cell using MSCP protected

SS foil. In addition, the MSCP protective layer can also be used to improve Li anode cycling performance in Li-sulfur cell (**Figure S15**).

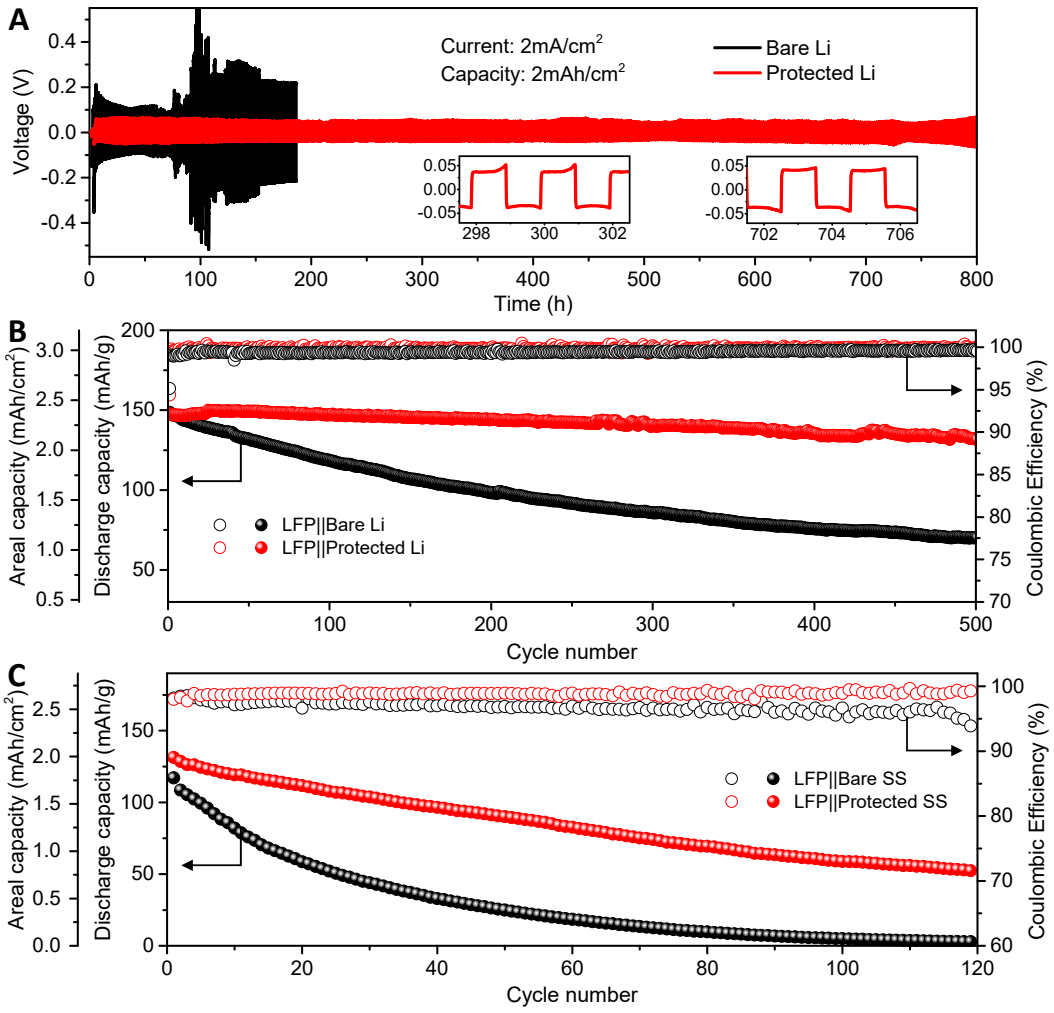

Figure 5. (A) Cycling performance of symmetric cells using bare (black) or MSCP protected (red) Li metal foils cycled at 2 mA cm^{-2} and 2 mAh cm^{-2}. (B) Cycling performance of Li||LFP full cells using bare (black) and MSCP protected (red) Li metal as anode at 0.5C (1C = 170 mAh/g). (C) Cycling performance of anode-free SS||LFP cells using bare SS foil (black) and MSCP protected (red) SS foil as anode at 0.5C.

In summary, an in-situ chemically cross-linked, multifunctional sulfur containing polymer protective layer has been demonstrated to show superior protection for Li metal anode. This protective layer on Li metal anode can facilitate forming a stable organic/inorganic hybrid SEI layer containing multiple components, such as polymer-tethered organo(poly)sulfide, inorganic Li_3PS_x and Li sulfides, and Li salts. Thanks to this protective robust SEI layer, dendrite-free Li deposition and dramatically enhanced cycling performance can be achieved for the Li plating/stripping cycling tests. Moreover, the protected Li metal anode enables an excellent cycling of symmetric cell and Li||LFP full cell (>89% capacity retention after 500 cycles and high average CE of 99.9%). The results show the superiority of this Li metal protection approach compared with strategies using Li_2S_8 or sulfur-rich polymer as additives. This proof-of-concept study in design of multicomponent hybrid protection layer can inspire new strategy in development of reactive polymeric composite SEI layer for Li metal anode. By a combination of interfacial chemistry, well-designed protective layer and advanced electrolyte systems, stable Li metal anodes for practical Li metal batteries could be achieved.

ASSOCIATED CONTENT

Supporting Information

The Supporting Information is available free of charge on the ACS Publications website at DOI: 10.1021/····

Experimental section, electrochemical measurements, characterization; ^{1}H-NMR spectra; XPS spectra; SEM images; Chemical structures; electrochemical data, Table summary and additional data analysis.

AUTHOR INFORMATION

Corresponding Author

*Email: dwang@psu.edu (Donghai Wang)

Author Contributions

‡ Y. Z. and G. L. contributed equally to this work.

Notes

The authors declare no competing interests.

ACKNOWLEDGMENT

This work was supported by the Assistant Secretary for Energy Efficiency and Renewable Energy, Office of Vehicle Technologies of the U.S. Department of Energy under Contract No. DE-EE0007795.

REFERENCES

(1) Guo, Y.; Li, H.; Zhai, T. Reviving Lithium-Metal Anodes for Next-Generation High-Energy Batteries. *Adv. Mater.* **2017,** 29, 1700007.

(2) Cheng, X.-B.; Huang, J.-Q.; Zhang, Q. Review—Li Metal Anode in Working Lithium-Sulfur Batteries. *J. Electrochem. Soc.* **2018,** 165, A6058-A6072.

(3) Cheng, X.-B.; Zhang, R.; Zhao, C.-Z.; Wei, F.; Zhang, J.-G.; Zhang, Q. A Review of Solid Electrolyte Interphases on Lithium Metal Anode. *Adv. Sci.* **2016,** 3, 1500213.

(4) Yamaki, J.-i.; Tobishima, S.-i.; Hayashi, K.; Keiichi, S.; Nemoto, Y.; Arakawa, M. A consideration of the morphology of electrochemically deposited lithium in an organic electrolyte. *J. Power Sources* **1998,** 74, 219-227.

(5) Peled, E. The Electrochemical Behavior of Alkali and Alkaline Earth Metals in Nonaqueous Battery Systems—The Solid Electrolyte Interphase Model. *J. Electrochem. Soc.* **1979,** 126, 2047-2051.

(6) Aurbach, D.; Zinigrad, E.; Cohen, Y.; Teller, H. A short review of failure mechanisms of lithium metal and lithiated graphite anodes in liquid electrolyte solutions. *Solid State Ionics* **2002,** 148, 405-416.

(7) Tripathi, A. M.; Su, W.-N.; Hwang, B. J. In situ analytical techniques for battery interface analysis. *Chem. Soc. Rev.* **2018,** 47, 736-851.

(8) Ding, F.; Xu, W.; Graff, G. L.; Zhang, J.; Sushko, M. L.; Chen, X.; Shao, Y.; Engelhard, M. H.; Nie, Z.; Xiao, J., et al. Dendrite-Free Lithium Deposition via Self-Healing Electrostatic Shield Mechanism. *J. Am. Chem. Soc.* **2013,** 135, 4450-4456.

(9) Zhang, H.; Eshetu, G. G.; Judez, X.; Li, C.; Rodriguez-Martínez, L. M.; Armand, M. Electrolyte additives for lithium metal anodes and rechargeable lithium metal batteries: progresses and perspectives. *Angew. Chem. Int. Ed.* **2018,** 57, 15002-15027.

(10) Gordin, M. L.; Dai, F.; Chen, S.; Xu, T.; Song, J.; Tang, D.; Azimi, N.; Zhang, Z.; Wang, D. Bis(2,2,2-trifluoroethyl) Ether As an Electrolyte Co-solvent for Mitigating Self-Discharge in Lithium–Sulfur Batteries. *ACS Appl. Mater. Interfaces* **2014,** 6, 8006-8010.

(11) Zhu, B.; Jin, Y.; Hu, X.; Zheng, Q.; Zhang, S.; Wang, Q.; Zhu, J. Poly(dimethylsiloxane) Thin Film as a Stable Interfacial Layer for High-Performance Lithium-Metal Battery Anodes. *Adv. Mater.* **2017,** 29, 1603755.

(12) Liu, W.; Lin, D.; Pei, A.; Cui, Y. Stabilizing Lithium Metal Anodes by Uniform Li-Ion Flux Distribution in Nanochannel Confinement. *J. Am. Chem. Soc.* **2016,** 138, 15443-15450.

(13) Li, N.-W.; Yin, Y.-X.; Yang, C.-P.; Guo, Y.-G. An Artificial Solid Electrolyte Interphase Layer for Stable Lithium Metal Anodes. *Adv. Mater.* **2016,** 28, 1853-1858.

(14) Zhang, X.-Q.; Cheng, X.-B.; Chen, X.; Yan, C.; Zhang, Q. Fluoroethylene Carbonate Additives to Render Uniform Li Deposits in Lithium Metal Batteries. *Adv. Funct. Mater.* **2017**, 1605989.

(15) Li, N.-W.; Yin, Y.-X.; Li, J.-Y.; Zhang, C.-H.; Guo, Y.-G. Passivation of Lithium Metal Anode via Hybrid Ionic Liquid Electrolyte toward Stable Li Plating/Stripping. *Adv. Sci.* **2017,** 4, 1600400.

(16) Adams, B. D.; Carino, E. V.; Connell, J. G.; Han, K. S.; Cao, R.; Chen, J.; Zheng, J.; Li, Q.; Mueller, K. T.; Henderson, W. A., et al. Long Term Stability of Li-S Batteries Using High Concentration Lithium Nitrate Electrolytes. *Nano Energy* **2017,** 40, 607-617.

(17) Yang, C.; Fu, K.; Zhang, Y.; Hitz, E.; Hu, L. Protected Lithium-Metal Anodes in Batteries: From Liquid to Solid. *Adv. Mater.* **2017,** 29, 1701169.

(18) Zheng, G.; Lee, S. W.; Liang, Z.; Lee, H.-W.; Yan, K.; Yao, H.; Wang, H.; Li, W.; Chu, S.; Cui, Y. Interconnected hollow carbon nanospheres for stable lithium metal anodes. *Nat. Nanotechnol.* **2014,** 9, 618-623.

(19) Wang, L.; Wang, Q.; Jia, W.; Chen, S.; Gao, P.; Li, J. Li metal coated with amorphous Li3PO4 via magnetron sputtering for stable and long-cycle life lithium metal batteries. *J. Power Sources* **2017,** 342, 175-182.

(20) Yan, K.; Lee, H.-W.; Gao, T.; Zheng, G.; Yao, H.; Wang, H.; Lu, Z.; Zhou, Y.; Liang, Z.; Liu, Z., et al. Ultrathin Two-Dimensional Atomic Crystals as Stable Interfacial Layer for Improvement of Lithium Metal Anode. *Nano Lett.* **2014,** 14, 6016-6022.

(21) Gao, Y.; Zhao, Y.; Li, Y. C.; Huang, Q.; Mallouk, T. E.; Wang, D. Interfacial Chemistry Regulation via a Skin-Grafting Strategy Enables High-Performance Lithium-Metal Batteries. *J. Am. Chem. Soc.* **2017,** 139, 15288-15291.

(22) Li, G.; Gao, Y.; He, X.; Huang, Q.; Chen, S.; Kim, S. H.; Wang, D. Organosulfide-plasticized solid-electrolyte interphase layer enables stable lithium metal anodes for long-cycle lithium-sulfur batteries. *Nat. Commun.* **2017,** 8, 850.

(23) Gao, Y.; Wang, D.; Li, Y. C.; Yu, Z.; Mallouk, T. E.; Wang, D. Salt-Based Organic–Inorganic Nanocomposites: Towards A Stable Lithium Metal/Li10GeP2S12 Solid Electrolyte Interface. *Angew. Chem. Int. Ed.* **2018,** 57, 13608-13612.

(24) Lopez, J.; Pei, A.; Oh, J. Y.; Wang, G.-J. N.; Cui, Y.; Bao, Z. Effects of Polymer Coatings on Electrodeposited Lithium Metal. *J. Am. Chem. Soc.* **2018,** 140, 11735-11744.

(25) Dong, T.; Zhang, J.; Xu, G.; Chai, J.; Du, H.; Wang, L.; Wen, H.; Zang, X.; Du, A.; Jia, Q., et al. A multifunctional polymer electrolyte enables ultra-long cycle-life in a high-voltage lithium metal battery. *Energy Environ. Sci.* **2018,** 11, 1197-1203.

(26) Zheng, G.; Wang, C.; Pei, A.; Lopez, J.; Shi, F.; Chen, Z.; Sendek, A. D.; Lee, H.-W.; Lu, Z.; Schneider, H., et al. High-Performance Lithium Metal Negative Electrode with a Soft and Flowable Polymer Coating. *ACS Energy Lett.* **2016,** 1, 1247-1255.

(27) Li, N.-W.; Shi, Y.; Yin, Y.-X.; Zeng, X.-X.; Li, J.-Y.; Li, C.-J.; Wan, L.-J.; Wen, R.; Guo, Y.-G. A Flexible Solid Electrolyte Interphase Layer for Long-Life Lithium Metal Anodes. *Angew. Chem. Int. Ed.* **2018,** 57, 1505-1509.

(28) Li, G.; Huang, Q.; He, X.; Gao, Y.; Wang, D.; Kim, S. H.; Wang, D. Self-Formed Hybrid Interphase Layer on Lithium Metal for High-Performance Lithium–Sulfur Batteries. *ACS Nano* **2018,** 12, 1500-1507.

(29) Lin, Z.; Liu, Z.; Fu, W.; Dudney, N. J.; Liang, C. Phosphorous Pentasulfide as a Novel Additive for High-Performance Lithium-Sulfur Batteries. *Adv. Funct. Mater.* **2013,** 23, 1064-1069.

(30) Lin, Z.; Liu, Z.; Fu, W.; Dudney, N. J.; Liang, C. Lithium Polysulfidophosphates: A Family of Lithium-Conducting Sulfur-Rich Compounds for Lithium–Sulfur Batteries. *Angew. Chem. Int. Ed.* **2013,** 52, 7460-7463.

(31) Li, W.; Yao, H.; Yan, K.; Zheng, G.; Liang, Z.; Chiang, Y.-M.; Cui, Y. The synergetic effect of lithium polysulfide and lithium nitrate to prevent lithium dendrite growth. *Nat. Commun.* **2015,** 6, 7436.

(32) Lu, Y.; Gu, S.; Hong, X.; Rui, K.; Huang, X.; Jin, J.; Chen, C.; Yang, J.; Wen, Z. Pre-modified Li3PS4 based interphase for lithium anode towards high-performance Li-S battery. *Energy Storage Mater.* **2018,** 11, 16-23.

(33) Wu, X.; El Kazzi, M.; Villevieille, C. Surface and morphological investigation of the electrode/electrolyte properties in an all-solid-state battery using a Li2S-P2S5 solid electrolyte. *J. Electroceram.* **2017,** 38, 207-214.

(34) Chen, S.; Dai, F.; Gordin, M. L.; Yu, Z.; Gao, Y.; Song, J.; Wang, D. Functional Organosulfide Electrolyte Promotes an Alternate Reaction Pathway to Achieve High Performance in Lithium–Sulfur Batteries. *Angew. Chem. Int. Ed.* **2016,** 55, 4231-4235.

(35) Li, G.; Sun, J.; Hou, W.; Jiang, S.; Huang, Y.; Geng, J. Three-dimensional porous carbon composites containing high sulfur nanoparticle content for high-performance lithium–sulfur batteries. *Nat. Commun.* **2016,** 7, 10601.

(36) Huang, H.; Zhong, B.; Zu, X.; Luo, H.; Lin, W.; Zhang, M.; Zhong, Y.; Yi, G. Fabrication of Ordered Nanopattern by using ABC Triblock Copolymer with Salt in Toluene. *Nanoscale Res. Lett.* **2017,** 12, 491.

(37) Zhao, C.-Z.; Cheng, X.-B.; Zhang, R.; Peng, H.-J.; Huang, J.-Q.; Ran, R.; Huang, Z.-H.; Wei, F.; Zhang, Q. Li2S5-based ternary-salt electrolyte for robust lithium metal anode. *Energy Storage Mater.* **2016,** 3, 77-84.

(38) Aurbach, D.; Pollak, E.; Elazari, R.; Salitra, G.; Kelley, C. S.; Affinito, J. On the Surface Chemical Aspects of Very High Energy Density, Rechargeable Li–Sulfur Batteries. *J. Electrochem. Soc.* **2009,** 156, A694-A702.

(39) Wang, X.; Gao, T.; Han, F.; Ma, Z.; Zhang, Z.; Li, J.; Wang, C. Stabilizing high sulfur loading Li–S batteries by chemisorption of polysulfide on three-dimensional current collector. *Nano Energy* **2016,** 30, 700-708.

(40) Parimalam, B. S.; Lucht, B. L. Reduction Reactions of Electrolyte Salts for Lithium Ion Batteries: LiPF6, LiBF4, LiDFOB, LiBOB, and LiTFSI. *J. Electrochem. Soc.* **2018,** 165, A251-A255.